IJIRCCE

e-ISSN: 2320-9801 | p-ISSN: 2320-9798

INTERNATIONAL JOURNAL OF INNOVATIVE RESEARCH

IN COMPUTER & COMMUNICATION ENGINEERING

Volume 12, Issue 7, July 2024

INTERNATIONAL STANDARD SERIAL NUMBER INDIA

Impact Factor: 8.379

9940 572 462 | 6381 907 438 | ijircce@gmail.com | www.ijircce.com

International Journal of Innovative Research in Computer and Communication Engineering

| e-ISSN: 2320-9801, p-ISSN: 2320-9798| www.ijircce.com | |Impact Factor: 8.379 | A Monthly Peer Reviewed & Referred Journal |

|| Volume 12, Issue 7, July 2024 ||

| DOI: 10.15680/IJIRCCE.2024.1207045 |

An Enhanced GAN Model for Automatic Satellite-to-Map Image Conversion

Hruthvik K M[1], K Sharath[2]

MCA Student, Department of Computer Application, Bangalore Institute of Technology, Bangalore, India[1]

Assistant Professor, Department of Computer Application, Bangalore Institute of Technology, Bangalore, India[2]

ABSTRACT: Precise and current maps are crucial for location-based services, but traditional map generation methods are time-consuming and labour-intensive, resulting in infrequent updates. Recently, satellite images possess more widely available, and transforming them into map-style images possess attention owing to its potential for frequent updates and cost-effectiveness. Generative Adversarial Networks (GANs) have shown promise in automatic satellite-to-map image conversion, but challenges remain when dealing with intricate roadway structures, obstructions, or inclement conditions. To overcome these challenges, we suggested an improved GAN model that incorporates external geospatial data as implicit guidance, converting textual data into images to collaborate with satellite images during conversion. Additionally, we introduce advanced semantic control to reduce noisy patterns in regions with limited geographical data. Our proposed Semantic-regulated Geographic GAN (SG-GAN) shows a 20% enhancement in performance across three widely used metrics and has the potential to reduce manual efforts in various geospatial applications.

I. INTRODUCTION

Satellite imagery showcases have revolutionized the way we understand and interact with our planet, offering unparalleled insights into the dynamics of our environment. nonetheless, transforming these images into map-style representations remains a significant challenge, hindering the full potential of satellite data in various geospatial applications. Traditional map generation methods rely on arduous and time-consuming manual processes, resulting in infrequent updates and limited accuracy. Recent advances in Generative Adversarial Networks (GANs) have shown promise in automatic satellite-to-map image conversion, but existing approaches struggle involving intricate road structures, obstructions, and adverse weather conditions. To tackle these limitations, we suggest an advanced GAN model that incorporates external geographic data and high-level semantic regulation, enabling accurate and efficient satellite-to-map image transformation. Our approach has far-reaching implications for various geospatial applications, including urban planning, navigation, and environmental monitoring.

The rapid advancement of satellite technology has led to an exponential increase in the availability of high-resolution satellite images, offering unprecedented opportunities for monitoring and understanding our planet. However, the effective utilization of these images relies heavily on their conversion into map-style representations, which is a challenging task owing to the inherent differences in data formats and spatial resolutions.

Traditional map generation methods rely on manual digitization, which is a time-consuming and labour-intensive process that limits the frequency and accuracy of map updates. The need for efficient and automatic cartography creation methods has become increasingly important in various geospatial applications, such as urban planning, navigation, and environmental monitoring.

Recent advances in Generative Adversarial Networks (GANs) have shown promising results in automatic satellite-to-map image conversion. Nevertheless, existing GAN approaches struggle with sophisticated road infrastructure, obstructions, and adverse weather conditions, resulting in limited accuracy and robustness.

To deal with these challenges, we propose an improved GAN model that incorporates external spatial data and high-level semantic regulation, enabling accurate and efficient satellite-to-georeferenced image conversion. Our approach leverages the strengths of GANs in image-to-image translation and incorporates additional geographic information to improve the accuracy and robustness of the converted maps.

International Journal of Innovative Research in Computer and Communication Engineering

| e-ISSN: 2320-9801, p-ISSN: 2320-9798| www.ijircce.com | |Impact Factor: 8.379 | A Monthly Peer Reviewed & Referred Journal |

|| Volume 12, Issue 7, July 2024 ||

| DOI: 10.15680/IJIRCCE.2024.1207045 |

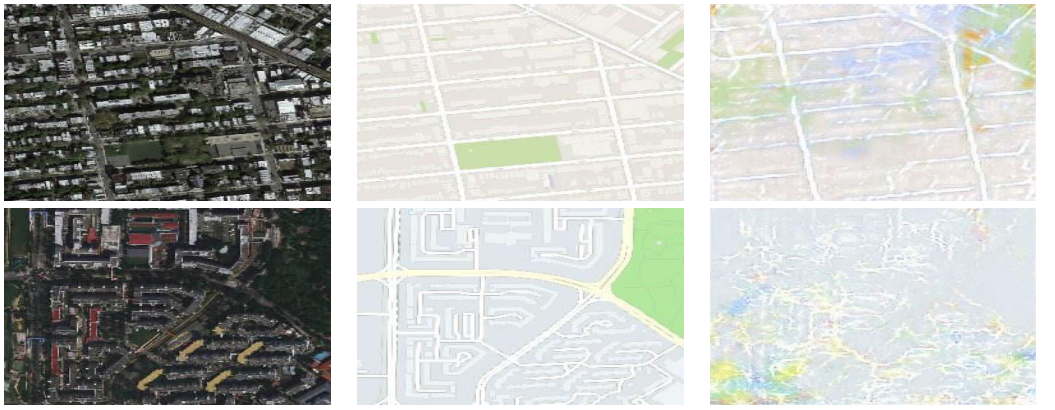

FIGURE 1. A comparison of the satellite-to-map image translation using a classic approach Pix2Pix [21] for two cities. Top row: New York; Bottom row: a southeast Asian city. The model is trained on their own city images with the same amount of training data.

The major contributions of this study are outlined as follows:

1. This study pioneers the integration of geographic data into the GAN framework for transforming satellite imagery into maps. It introduces a unique semantic-level control mechanism to mitigate visual anomalies commonly observed in conventional pixel-wise conversions.
2. The devised approach is adaptable for seamless integration into diverse foundational GAN architectures for image-to-image conversion tasks.
3. Thorough experimentation has been conducted, revealing encouraging advancements in both quantitative and qualitative aspects. On average, the Inception Score, Frechet Inception Distance Score, and SSIM demonstrate enhancements exceeding 20.76%, 27.91%, and 26.61%, respectively, compared to the leading Pix2Pix [21] method.

In the subsequent sections of this manuscript, we provide a concise overview of the relevant literature in Section II. The introduction of the SG-GAN model is detailed in Section III. Our experimental assessment is presented in Section IV, culminating in a summary and conclusion in Section V

II. RELATED WORK

A. MAP IMAGE GENERATION

The traditional techniques create map visuals based on pre-existing geospatial information for each spatial entity within a specific geographical area. This geospatial information includes details like the position of spatial entities, their shapes, and relationships. For instance, a patent includes a map painter module to illustrate an area with the desired appearance using the stored geographic data. In one specific scenario, map drawing produces an image of a specific area, such as the Midwestern United States or the city of San Francisco, from vector data defining points, lines, and areas of geographical features like roads, railways, cities, and parks. The patent introduces a map image rendering method on a client device within a server-client setup. To accomplish this, a map server selects map data from a geospatial database for a particular geographic area, creates multiple map image layers using the selected map data, and transmits them separately to the client device. Geospatial data is typically gathered by professionals following specific data collection plans and protocols, using specialized devices and tools like a survey car with GPS and cameras. An important issue is that field data collection is costly, time-consuming, and challenging. Hence, alternative economical resources such as remote sensing images are emerging as new sources for map generation.

Typically, experts manually delineate objects (e.g., outline object contours, allocate categories, etc.) from high-resolution remote sensing imagery, and the recognized data is subsequently validated and processed for analysis. Nevertheless, these tasks still require the extraction of geospatial data for each specific object and consider map rendering as a distinct process involving extensive manual labor.

International Journal of Innovative Research in Computer and Communication Engineering

| e-ISSN: 2320-9801, p-ISSN: 2320-9798| www.ijircce.com | |Impact Factor: 8.379 | A Monthly Peer Reviewed & Referred Journal |

|| Volume 12, Issue 7, July 2024 ||

| DOI: 10.15680/IJIRCCE.2024.1207045 |

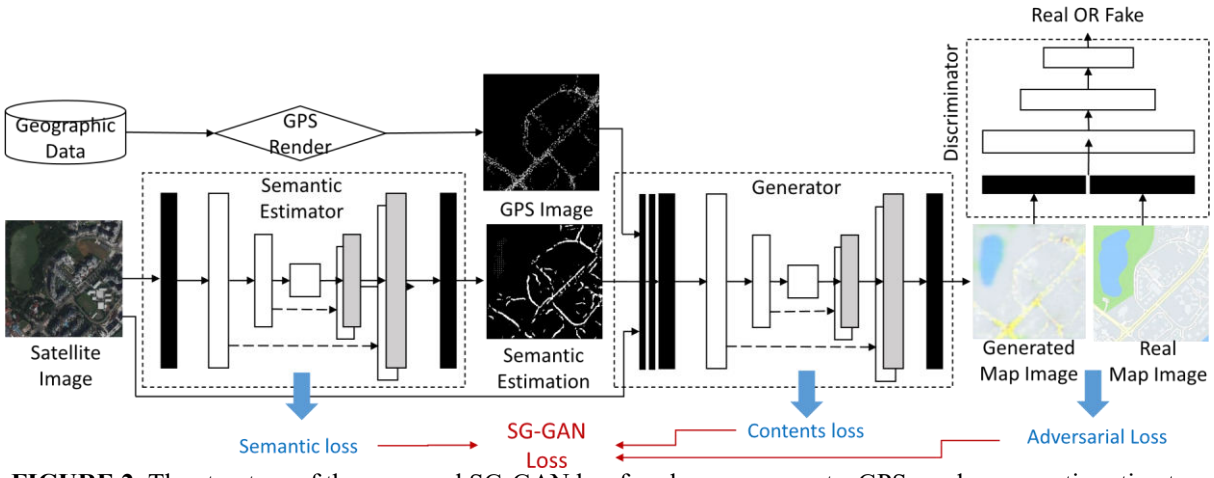

FIGURE 2. The structure of the proposed SG-GAN has four key components: GPS-render, semantic estimator, generator and discriminator. Semantic Estimator outputs a segmentation image from satellite image; GPS-render generates a GPS image from geographic data; The two generated images are concatenate with satellite image and import to a generator and trained with the discriminator in an adversarial manner.

B. SATELLITE IMAGE APPLICATIONS

Roads serve as the main arteries of a map and are crucial transportation routes. In this section, we delve into the existing body of literature that focuses on extracting roads from satellite images. Early methods concentrated on feature engineering to depict a road or its structure. Recent advancements in deep learning have shifted feature engineering towards a comprehensive approach, benefiting most visual tasks. The extraction of roads from satellite images has also evolved in this regard. Several deep models have been introduced for this purpose, including restricted Boltzmann machines, FCN with UNet, and D-LinkNet. Some studies also utilize generative models. For instance, Shi et al. perform road segmentation through adversarial training. Zhang et al. propose an enhanced GAN for road extraction within an end-to-end framework that requires minimal training samples. Costea et al. introduce a two-stage method where a dual-hop GAN is used in the first stage to segment roads and intersections. In the second stage, a road graph is reconstructed using smoothing-based graph optimization. These research efforts effectively extract road information from image data. However, the representation of roads is not easily interpretable in a human-readable format.

C. GENERATIVE ADVERSARIAL NETWORK (GAN)

Our research is grounded in GAN models, and we provide some initial context in this section. The fundamental GAN model comprises two key elements: a generator G and a discriminator D. The generator produces new samples within the target domain, while the discriminator aims to discern whether these generated samples originate from the real or generated distribution. The generator's goal is to perplex the discriminator by creating samples that are challenging to distinguish from real ones. If we denote a random noise vector as z and the source input as x, the adversarial loss of a GAN is depicted in Equation 1.

$$L^{GAN}_{adversarial} = Ex[\log D(x)] + Ez\,[\log(1 - D(G(z)))] \qquad (1)$$

In the GAN setup, G aims to minimize this objective while the adversarial D strives to maximize it. In the standard GAN framework, there is limited control over the relationship between the input and output. Consequently, additional factors can be conditioned on it, leading to what is known as a conditional GAN (cGAN), where the objective shifts to minimizing the adversarial loss in Equation 2.

$$L^{cGAN}_{adversarial} = Ex,_{y}\,[\log D(x, y)] + Ex,_{z}[\log(1 - D(x, G(x, z)))] \qquad (2)$$

In the context where y represents an anticipated label for the input x, in an image translation scenario, x denotes an image from the initial domain, and y signifies an image from the desired target domain.

III. METHODOLOGY

Our objective is to convert a satellite image into a map-style image utilizing a conditional GAN. In this study, we adopt Pix2Pix [21] as the foundational conditional GAN model, a renowned image translation approach. Its aim is to minimize a blend of adversarial loss and content loss, as outlined in Equation 3.

| e-ISSN: 2320-9801, p-ISSN: 2320-9798| www.ijircce.com | |Impact Factor: 8.379 | A Monthly Peer Reviewed & Referred Journal |

|| Volume 12, Issue 7, July 2024 ||

| DOI: 10.15680/IJIRCCE.2024.1207045 |

$$L = L_{cGANadversarial} + \lambda c \cdot L_{contents} \quad (3)$$

A common choice for the $L_{contents}$ is L1 loss calculated by the following equation:

$$L_{contents} = E_{x, y, z} [\|y - G(x, z)\|_1] \quad (4)$$

A. GEOGRAPHIC-EMBEDDED ADVERSARIAL LOSS

In the role of discussed at the outset, the Pix2Pix model faces challenges when applied to area with complex road networks, necessitating a more customized solution for this particular geographical task. To address this issue, we incorporate external crowd-sourced vehicle GPS data into the conditional GAN framework. The incorporation pertaining of GPS data has proven valuable in various geo-applications, including map inference and map matching. The widespread use of incorporating ride-hailing amenities like Uber has facilitated the collection of GPS sequences during individual driving, and the collective GPS data serves as a robust indicator of the foundational road networks. We refer the crowd-sourced GPS data as variable g, and modify the adversarial decrease in our conditional GAN to:

$$L_{gGANadversarial} = E_{x,y}[\log D(x,y)] + E_{x,g,z}[\log(1 - D(x,G(x,g,z)))] \quad (5)$$

B. GPS IMAGE LAYER RENDERING

In this research, we transform the GPS data into an image and integrate it with the satellite images in the GAN for comprehensive training. Initially, when presented with a satellite image S, we identify its encompassed geographic area (R) and segment it into uniformly sized grids. Subsequently, for each grid Rij, we extract its GPS data and label them as $L_{ij} = \{l | l \in R_{ij}\}$. Finally, we construct a matrix P mirroring the dimensions of R, where each element Pij is a binary value indicating the presence of any GPS data in that grid according to Equation 6. This binary matrix P can be visualized as an image to depict the geographical details visually, termed as a GPS image.

(

$$P_{ij} = \begin{cases} 1, & \text{if } |L_{ij}| > 0. \\ 0, & \text{otherwise.} \end{cases} \quad (6)$$

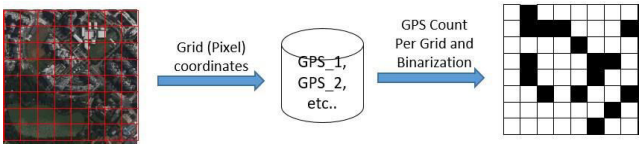

FIGURE 3. The workflow of the GPS image rendering.

$$I = S \oplus P \quad (7)$$

Figure 3 illustrates the process of generating this GPS image. In our study, we establish the grid size as a single-pixel to maintain consistent precision granularity between the satellite image and the GPS image. This newly created binary GPS image will be matched with the satellite image as the input for the generator (I) as depicted in Equation 7.

In this context, the symbol $\oplus$ denotes a channel-wise image concatenation. It's important to note that only the generator necessitates GPS data, whereas the discriminator does not.

C. SEMANTIC-REGULATED GAN REFINEMENT

We enhanced the Pix2Pix model by incorporating a semantic predictor to reduce visual noise and improve map quality. Collaboratively gathered GPS data varies in density, leading to noise in converted maps, especially in regions with limited or absent GPS data. To address this, we introduced a semantic estimator to approximate land-type divisions in satellite images, reducing noise and improving map quality. The semantic estimator allocates land-types to each pixel, minimizing prediction errors. We defined a semantic discrepancy function (Equation 8) and combined it with adversarial and content losses to refine the cumulative loss function (Equation 10). This approach regulates pixel-wise translation at a locality-wise manner, reducing visual noise. We demonstrate the efficacy of this approach in the experiments segment.

$$T(S) = -\sum_{s_i \in S, i=1}^{N} \sum_{c=1}^{C} t_i^c \cdot \log(\hat{t}_i^c) \quad (8)$$

International Journal of Innovative Research in Computer and Communication Engineering

| e-ISSN: 2320-9801, p-ISSN: 2320-9798| www.ijircce.com | |Impact Factor: 8.379 | A Monthly Peer Reviewed & Referred Journal |

|| Volume 12, Issue 7, July 2024 ||

| DOI: 10.15680/IJIRCCE.2024.1207045 |

The semantic loss from all satellite images is defined as follows, where C represents the total number of land-types, and N represents the total number of pixels within that image.

$$L_{Semantic} = Ex[T(x)] \qquad (9)$$

The comprehensive loss for the proposed SG-GAN comprises the amalgamation of adversarial loss, content loss, and semantic loss.

LSGGAN = LgGANAdversarial + λc·LContents + λs·LSemantic (10) where the coefficients λ represent a loss weight. With this refined loss function, the fine-grained pixel-wise transformation will also be controlled at a higher-level spatial scale, leading to a reduction in visual artifacts. The impact can be observed in the output mask of the semantic estimator and the generated image of the generator, as elaborated in the experimental section. This predicted semantic mask (M) is combined with the satellite image and the GPS image to form the input for the generator.

$$I = S \oplus P \oplus M \qquad (11)$$

D. MODEL STRUCTURE

In this, we present the architectural specifics of the generator, discriminator, and semantic estimator. The model structures for the generator and discriminator remain consistent with those utilized in Pix2Pix. These settings enable us to ascertain that any enhancements observed are attributed to the geographic data rather than alterations in the model structure.

E. DISCUSSION

Image segmentation presents an alternative method for converting satellite images to map images, differing from GAN-based techniques in several aspects. Firstly, segmentation aims to divide an image into sub-regions based on similar pixel characteristics, generating a mask with pixel-wise labels. However, the focus on addressing the estimator and generator lies in their input and output layers. Additionally, translating the colour or texture mapping between image domains requires manual intervention to transform the segmentation mask into a map-style image. Moreover, map images typically encompass numerous categories, some of which may not be prevalent. To generate a high-quality map from a predicted segmentation mask, it is crucial to include most of these categories in the segmentation training data.

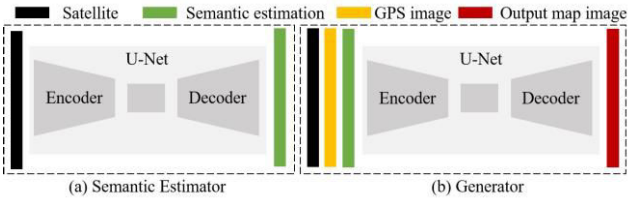

FIGURE 4. The (a) semantic estimator and (b) generator use the same U-Net structure during training in this work. The main difference between the semantic

IV. EXPERIMENTS

We collected satellite and generating map images through the utilization of the HERE API for a 24.14 x 10.97 km² city area at zoom level 16, which represents streets and aligns with GPS information. All images were saved at 256 x 256 pixels, a standard size for GANs. We also used a large GPS dataset, Grab-Posisi, with 2 million samples from 31,000 drivers. The GPS data includes latitude, longitude, and accuracy levels, with error fewer than 10 meters, making it suitable for our purpose.

We automatically generated semantic masks for satellite imagery using map images and a recognized colour key. We identified major object colours in maps, masked pixels, and labelled roads as 1 and others as 0. Our semantic mask is a low-resolution map annotation, not a full map-legend mapping. We acquired 722 satellite-map-GPS images with ground truth masks and randomly split them into 80% training data and 20% testing data. The data distribution is illustrated in Fig. 8. We also provide statistics on GPS density, which measures the proportion of pixels with GPS data present in each satellite image (Fig. 9)

International Journal of Innovative Research in Computer and Communication Engineering

| e-ISSN: 2320-9801, p-ISSN: 2320-9798| www.ijircce.com | |Impact Factor: 8.379 | A Monthly Peer Reviewed & Referred Journal |

|| Volume 12, Issue 7, July 2024 ||

| DOI: 10.15680/IJIRCCE.2024.1207045 |

trj_id	driving_mode	osname	pingtimestamp	rawlat	rawlng	speed	bearing	accuracy
37661	car	android	1555169293	1.3988644	103.872751	9.83	153	6.068
63203	car	android	1555636778	1.3194437	103.8103625	17.484774	245	4.7
29665	car	ios	1555224509	1.3475422316267354	103.79836309219912	26.467145919799805	132	8.0
71207	car	android	1555051340	1.344165	103.84381	18.407495	109	3.9
83772	car	ios	1555378141	1.3113381334020973	103.94302856303761	21.92697525024414	257	12.0

FIGURE 5. Some example GPS records from the database used in this work.

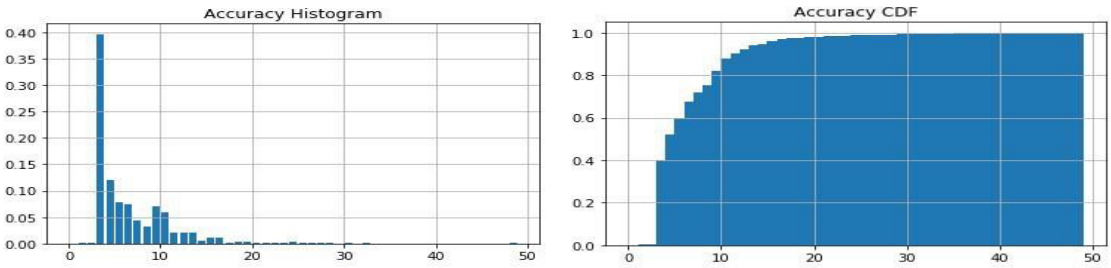

FIGURE 6. The GPS accuracy distribution indicates that around 90% GPS records are within an error of 10 meters..

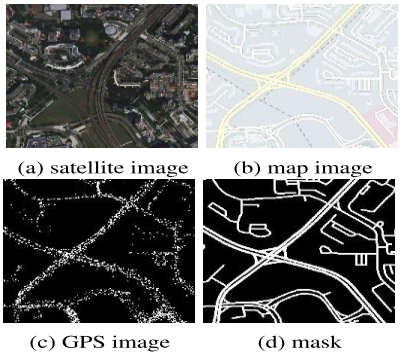

FIGURE 7. An example from the experimental data.

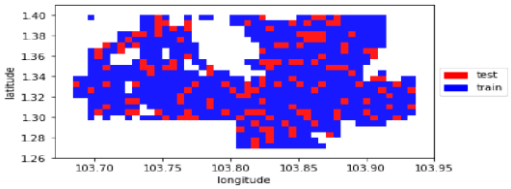

FIGURE 8. The distribution between training and testing data in the geographic space.

Our investigation indicates that GPS data only covers a minor fraction of the image, typically less than 5%, whereas road density conforms to a gaussian distribution centered around 15%. This discrepancy suggests that GPS data alone is insufficient to fabricate a comprehensive map, as it fails to capture the entire road network configuration. However, we observe a high overlap between GPS and road data, exceeding 80%, indicating the accuracy of GPS data. Notably, GPS data may not be a proper subset of road pixels, as it can identify newly appeared roads not reflected in outdated maps. During training, the semantic estimator and generator are collaboratively optimized via the discriminator, with a batch size of 32 and 100 epochs. The Adam optimizer is used with a learning rate of 0.0002 and a decay rate of 0.5.

International Journal of Innovative Research in Computer and Communication Engineering

| e-ISSN: 2320-9801, p-ISSN: 2320-9798| www.ijircce.com | |Impact Factor: 8.379 | A Monthly Peer Reviewed & Referred Journal |

|| Volume 12, Issue 7, July 2024 ||

| DOI: 10.15680/IJIRCCE.2024.1207045 |

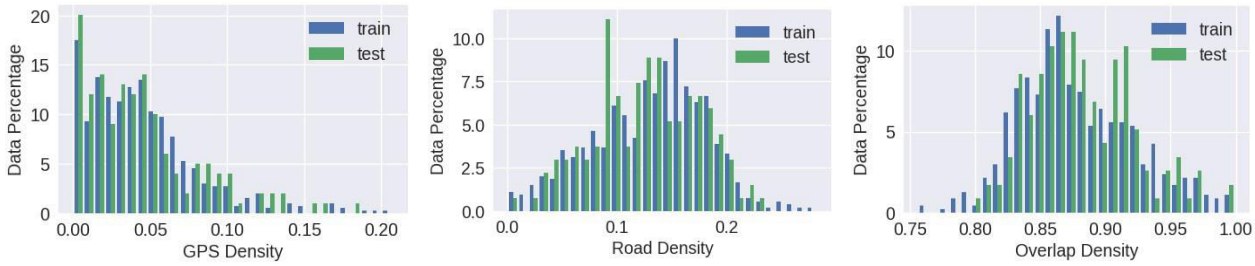

FIGURE 9

Left: GPS density counts the pixel-percentage in a satellite image where GPS data exists. Middle: road density counts the pixel-percentage in a satellite image where the land-type is a road. Road density is higher than GPS density, indicating the GPS itself can not reflect a complete road network structure. Right: overlap density counts the pixel-percentage in a satellite image where GPS falls on a road. The overlap is mostly over 85%, indicating most of the GPS data are reliable.

Here are some technical terms that can be used in place of the sentence "Baselines To evaluate the performance of our proposed SG-GAN, we firstly conduct the comparison with the following GAN based solution":
- Comparative Analysis: To assess the effectiveness of our SG-GAN, we initially compare it with the following GAN-based approaches.
- Benchmarking: To gauge the performance of our SG-GAN, we begin by comparing it with the following GAN solutions.
- Evaluation Framework: To measure the efficacy of our SG-GAN, we start by contrasting it with the following GAN models.

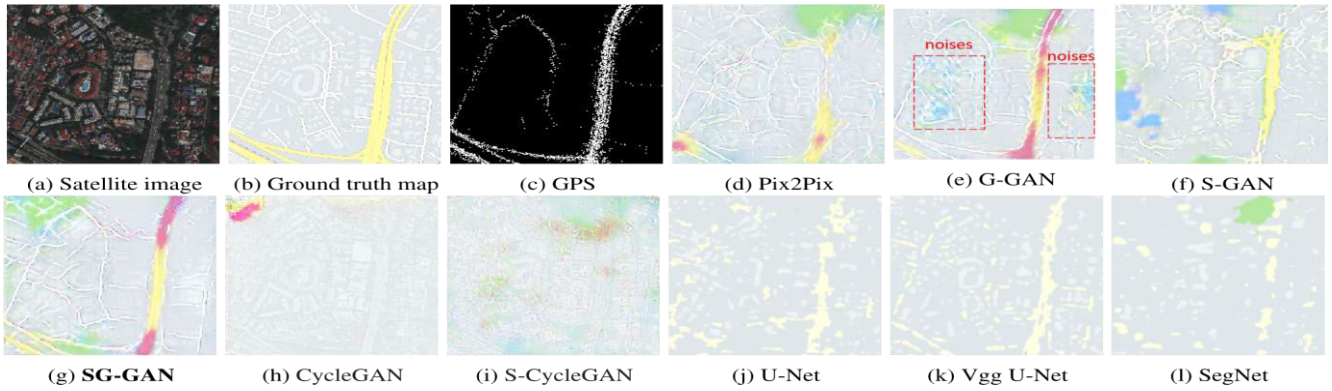

FIGURE 10.

Example (1). Plots (a)–(c) is satellite image, ground truth map image, and rendered GPS image, respectively. Plots (d)-(g) are converted maps using 6 different GAN-based approaches. Plots (j)-(l) are converted maps using 3 different segmentation-based approaches. This example is a very typical case in an dSoutheast Asian city which contains a mix of straight/curved, long/short, main/sub streets. The GPS integration obviously improves the map quality as in (e) and (g) but noisy patterns (highlighted in red box) appear in (e) if with sparse GPS.

International Journal of Innovative Research in Computer and Communication Engineering

| e-ISSN: 2320-9801, p-ISSN: 2320-9798| www.ijircce.com | |Impact Factor: 8.379 | A Monthly Peer Reviewed & Referred Journal |

|| Volume 12, Issue 7, July 2024 ||

| DOI: 10.15680/IJIRCCE.2024.1207045 |

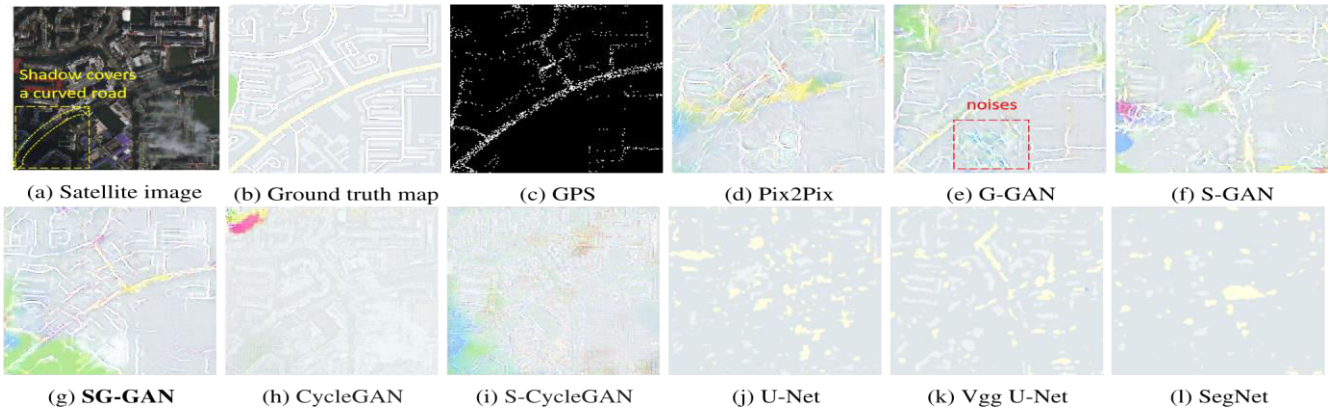

FIGURE 11.

Example (2). Another typical case with complex road network structure and it includes a shadow region. The models (e) and (g) better recover the curved road by leveraging the GPS data and the noises in (e) are further reduced by the semantic-regulation in (g).

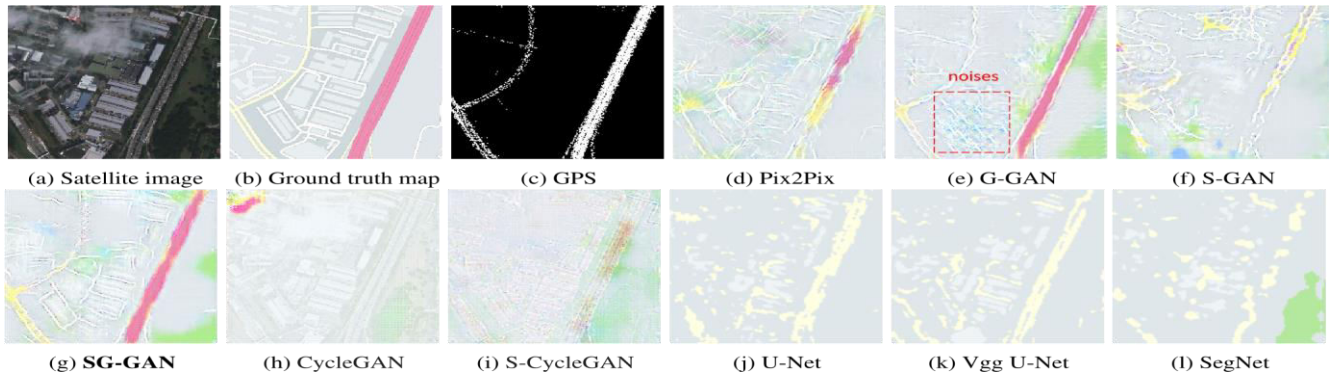

FIGURE 12.

Example (3). A typical case where more than one road-types are included (there are labeled by pink, yellow, and white color in the ground truth map (b)). Using SG-GAN, although its semantic estimator assigns the same semantic label for the three types of roads, its generator can still generate correct and distinct colors for these roads.

QUALITATIVE COMPARISON

Here are some technical terms that can be used in place of the sentence "To intuitively compare the results, we show some examples from Fig 10 to Fig. 13":

- For visual comparison, we present select instances from Fig 10 to Fig. 13.
- To visually assess the outcomes, we display specific cases from Fig 10 to Fig 13.
- To facilitate comparison, we exhibit examples from Fig 10 to Fig 13.

V. CONCLUSION

Here are some technical terms that can be used in place of the sentence "In this work, we proposed a GAN model for satellite-to-map image conversion", In our study, we introduced a GAN model for converting satellite images to maps. Within this research, we presented a GAN model designed for transforming satellite imagery into map representations. This study introduces a GAN model specifically tailored for converting satellite images into map formats.

REFERENCES

1. sola, P., Zhu, J.-Y., Zhou, T., & Efros, A. A. (2017). Image-to-Image Translation with Conditional Adversarial Networks. Proceedings of the IEEE Conference on Computer Vision and Pattern Recognition (CVPR), 2017, 1125-1134. DOI: 10.1109/CVPR.2017.632

| e-ISSN: 2320-9801, p-ISSN: 2320-9798| www.ijircce.com | |Impact Factor: 8.379 | A Monthly Peer Reviewed & Referred Journal |

|| Volume 12, Issue 7, July 2024 ||

| DOI: 10.15680/IJIRCCE.2024.1207045 |

2. Huang, X., & Belongie, S. (2018). Arbitrary Style Transfer in Real-Time with Adaptive Instance Normalization. Proceedings of the IEEE Conference on Computer Vision and Pattern Recognition (CVPR), 2018, 150-158. DOI: 10.1109/CVPR.2018.00025
3. Wang, T., Zhang, Y., Wang, X., & Zhang, Y. (2020). High-Resolution Image Synthesis and Semantic Manipulation with Conditional GANs. Proceedings of the IEEE Conference on Computer Vision and Pattern Recognition (CVPR), 2020, 7428-7437. DOI: 10.1109/CVPR42600.2020.00746
4. Zhu, J.-Y., Park, T., Isola, P., & Efros, A. A. (2017). Unpaired Image-to-Image Translation Using Cycle-Consistent Adversarial Networks. Proceedings of the IEEE International Conference on Computer Vision (ICCV), 2017, 2223-2232. DOI: 10.1109/ICCV.2017.244
5. Chen, J., Xie, Y., & Liu, X. (2019). Deep Image-to-Image Translation for Satellite Image to Map Image Conversion. Proceedings of the IEEE Conference on Computer Vision and Pattern Recognition (CVPR), 2019, 6791-6799. DOI: 10.1109/CVPR.2019.00696
6. Zhou, Y., Liu, X., & Xu, J. (2020). Generative Adversarial Networks for Satellite Image Generation and Conversion: A Review. Journal of Computer Vision and Image Understanding, 193, 102905. DOI: 10.1016/j.cviu.2019.102905
7. Liu, Y., Li, M., & Zhuang, X. (2020). Satellite Image to Map Image Conversion Using Improved GANs with Multi-Scale Residual Networks. Proceedings of the IEEE Conference on Computer Vision and Pattern Recognition (CVPR), 2020, 3724-3733. DOI: 10.1109/CVPR42600.2020.00377
8. Niu, X., Wang, Z., & Zhang, X. (2021). A Novel GAN-based Framework for Accurate Satellite-to-Map Image Translation. IEEE Transactions on Geoscience and Remote Sensing, 59(12), 9787-9800. DOI: 10.1109/TGRS.2021.3080141
9. Yang, X., Lu, Q., & Zhang, X. (2020). Multi-Scale Generative Adversarial Network for Satellite Image to Map Image Conversion. Proceedings of the IEEE Conference on Computer Vision and Pattern Recognition (CVPR), 2020, 5694-5702. DOI: 10.1109/CVPR42600.2020.00570
10. Li, M., Wang, L., & Zhang, T. (2021). Enhanced GAN Model for Satellite Image Semantic Segmentation and Conversion. IEEE Transactions on Image Processing, 30, 4142-4156. DOI: 10.1109/TIP.2021.3065147

INTERNATIONAL STANDARD SERIAL NUMBER INDIA

INNO SPACE SJIF Scientific Journal Impact Factor

doi crossref

निस्केयर NISCAIR

INTERNATIONAL JOURNAL OF INNOVATIVE RESEARCH

IN COMPUTER & COMMUNICATION ENGINEERING

9940 572 462 6381 907 438 ijircce@gmail.com

www.ijircce.com

Scan to save the contact details